

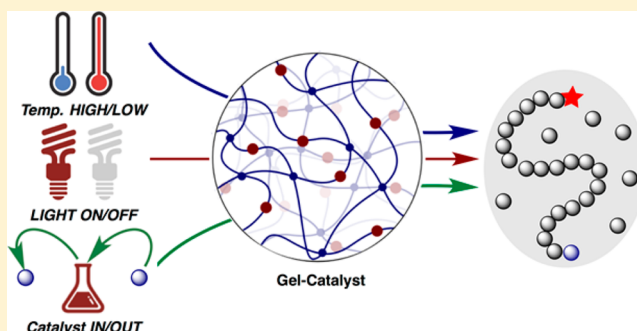
# Logic-Controlled Radical Polymerization with Heat and Light: Multiple-Stimuli Switching of Polymer Chain Growth via a Recyclable, Thermally Responsive Gel Photoredox Catalyst

Mao Chen,<sup>†</sup> Shihong Deng, Yuwei Gu, Jun Lin,<sup>‡</sup> Michelle J. MacLeod, and Jeremiah A. Johnson<sup>\*‡</sup>

Department of Chemistry, Massachusetts Institute of Technology, Cambridge, Massachusetts 02139, United States

## Supporting Information

**ABSTRACT:** Strategies for switching polymerizations between “ON” and “OFF” states offer new possibilities for materials design and fabrication. While switching of controlled radical polymerization has been achieved using light, applied voltage, allosteric effects, chemical reagents, pH, and mechanical force, it is still challenging to introduce multiple external switches using the same catalyst to achieve logic gating of controlled polymerization reactions. Herein, we report an easy-to-synthesize thermally responsive organo-/hydro-gel that features covalently bound 10-phenylphenothiazine (PTH). With this “Gel-PTH”, we demonstrate switching of controlled radical polymerization reactions using temperature “LOW”/“HIGH”, light “ON”/“OFF”, and catalyst presence “IN”/“OUT”. Various iniferters/initiators and a wide range of monomers including acrylates, methacrylates, acrylamides, vinyl esters, and vinyl amides were polymerized by RAFT/iniferter and ATRP methods using Gel-PTH and a readily available compact fluorescent light (CFL) source. In all cases, polymer molar masses increased linearly with conversion, and narrow molar mass distributions were obtained. To further highlight the utility of Gel-PTH, we achieved “AND” gating of controlled radical polymerization wherein various combinations of three stimuli were required to induce polymer chain growth. Finally, block copolymer synthesis and catalyst recycling were demonstrated. Logic-controlled polymerization with Gel-PTH offers a straightforward approach to achieve multiplexed external switching of polymer chain growth using a single catalyst without the need for addition of exogenous reagents.



## INTRODUCTION

The use of external stimuli to switch controlled radical polymerization (CRP) between “ON” and “OFF” states has attracted significant attention in recent years.<sup>1–3</sup> Such methods not only allow for the preparation of polymers with desired architectures and molecular weights, but also provide opportunities to manipulate reactions temporally, spatially, and orthogonally to other processes. Fundamental innovations guided by deep mechanistic insights have enabled “ON” and “OFF” switching of CRP using light,<sup>3–6</sup> applied voltage,<sup>7,8</sup> allosteric effects,<sup>9</sup> chemical reagents,<sup>10–13</sup> and mechanical force<sup>14,15</sup> (Figure 1).

Since the earliest reports of photoinduced CRP,<sup>16</sup> light has been widely adopted as the stimulus-of-choice thanks to its convenience, simplicity, low cost, etc.<sup>3–6</sup> Photo-CRP variants of atom transfer radical polymerization (ATRP),<sup>17–33</sup> reversible addition–fragmentation chain transfer polymerization (RAFT) and related iniferter polymerization,<sup>34–46</sup> Co-mediated CRP,<sup>47,48</sup> Te-mediated CRP,<sup>49,50</sup> and other mechanisms<sup>51–55</sup> have been successfully developed. These methods operate through either intramolecular primary photochemical processes (e.g., bond homolysis) or intermolecular photoinduced single electron transfer (SET) or energy transfer. The latter class enables “ON”/“OFF” control of polymer chain growth through

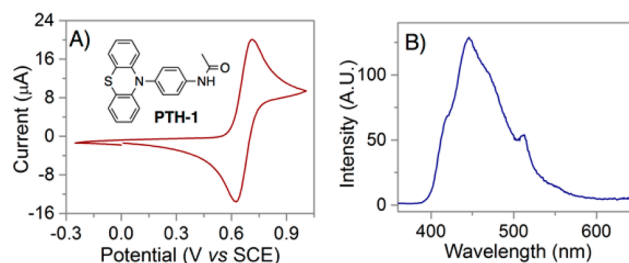


**Figure 1.** Characterization of the model catalyst PTH-1. (A) Cyclic voltammetry conducted using 0.1 M tetrabutylammonium hexafluorophosphate as electrolyte in acetonitrile (MeCN) at 25 °C. (B) Fluorescence spectrum of PTH-1 in MeCN at 25 °C.

photoactivation of a suitable photoredox catalyst;<sup>3,4,43</sup> the polymer chain itself does not need to absorb light. For example, Fors and Hawker reported on the use of an Ir-based photoredox catalyst to achieve visible light CRP in 2012.<sup>17,18</sup> Later, the same group also reported the synthesis of similar polymers using 10-phenylphenothiazine (PTH) as an organic

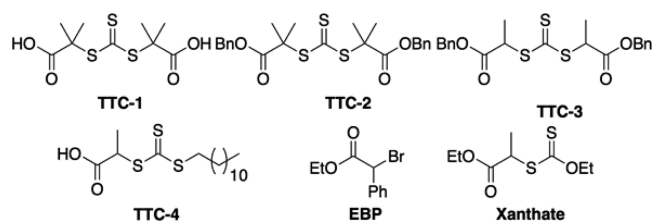
Received: October 3, 2016

photocatalyst.<sup>19</sup> The Matyjaszewski group systematically studied the mechanism of this so-called “metal-free ATRP” reaction.<sup>20,21</sup> They disclosed that the success of *N*-aryl phenothiazine photocatalysts (e.g., PTH) relies on the ability of these compounds to undergo both fast initiation/activation and efficient deactivation.<sup>21</sup> Miyake and co-workers have shown that phenazines, which absorb more strongly than PTH above 400 nm, are also outstanding photocatalysts for metal-free ATRP.<sup>33</sup> The Boyer group has developed robust and versatile photoredox CRPs that utilize RAFT agents as iniferters and various photoredox catalysts; these systems have been adapted to provide features such as oxygen tolerance,<sup>35,36</sup> tacticity-control,<sup>38</sup> catalyst/iniferter selectivity,<sup>39</sup> and infrared light reactivity.<sup>44</sup>

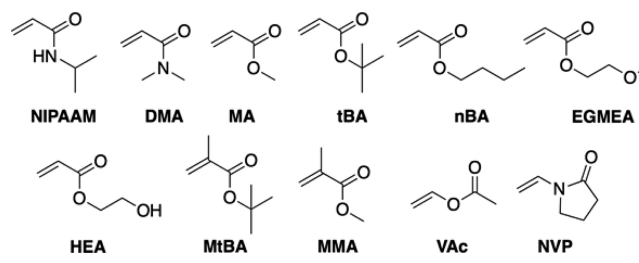
Biological systems also regulate polymer growth in response to external stimuli; however, rather than relying on a single stimulus, nature integrates signals from multiple stimuli (e.g., light, temperature, availability of resources, etc.). In synthetic systems, though multiple-wavelength-selective reactions have been reported,<sup>51</sup> to our knowledge there are no reports of using multiple external stimuli of different types to control CRP. Very recently, Boyer and co-workers reported on the development of a CRP method that was gated using light and pH; however, the authors needed to physically add acid or base to the reaction to switch the polymerization.<sup>46</sup> The realization of truly eternally regulated “logic-controlled polymerization” (Logic-CRP) has not, to our knowledge, been achieved. Logic-CRP would represent a step toward mimicking natural biopolymer synthesis and potentially open unprecedented materials fabrication opportunities. We envisioned that such externally switchable Logic-CRP could be realized through the development of a transparent, stimuli-responsive heterogeneous photocatalyst.

Herein, we report our design of a thermally responsive gel with covalently bonded PTH photocatalyst: “Gel-PTH”. When swollen in an appropriate solvent, Gel-PTH provides a transparent heterogeneous catalyst framework for photoredox CRP. In addition to “ON”/“OFF” control using light, the thermally responsive nature and excellent mechanical properties of Gel-PTH enable switching of CRP using temperature as a second external control and catalyst presence as a physical intervention control, respectively, thus enabling externally regulated “AND” gating of CRP. Furthermore, based on the ability to physically remove the catalyst, we demonstrate efficient catalyst recycling over six cycles with no decrease in polymerization rate. Finally, we show that Gel-PTH is effective for photoredox catalyzed CRP from trithiocarbonates (TTCs) and xanthates (photoiniferter/RAFT) and ethyl 2-bromopropionate (EBP) (photo-ATRP) using a wide range of monomers including acrylates, methacrylates, acrylamides, vinyl esters, and vinyl amides (Scheme 1 and Scheme 2).

Scheme 1. Chemical Structures of Iniferters/Initiators



Scheme 2. Chemical Structures of Monomers



## RESULTS AND DISCUSSION

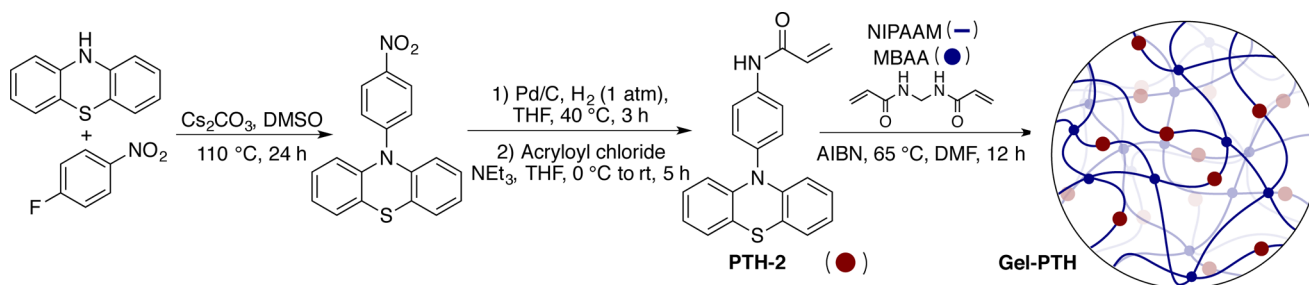
**1. Synthesis and Characterization of Gel-PTH.** To incorporate PTH into a polymer network, a *para*-acrylamide substituent was installed onto the 10-phenyl ring of PTH to provide PTH-2 (Scheme 3). Polymerization of PTH-2 would produce poly(acrylamide) with PTH groups linked to the polymer backbone via an amide. Thus, to investigate the impact of this amide linkage on the properties of PTH, we first synthesized 4-acetamide-PTH (PTH-1) as a model compound to study the electrochemistry and photochemistry of our target catalyst (Scheme S1). The Hammett substituent constant for *para*-acetamide is  $\sigma_p = 0.00$ , which suggests that this substituent should have little effect on the properties of PTH.<sup>56</sup> Indeed, the oxidation potential for conversion of PTH-1 to PTH-1<sup>•+</sup> as measured by cyclic voltammetry (CV) was  $E^{\text{ox}} = +0.68$  V vs. SCE (Figure 1A), which is the same value observed for the parent molecule PTH. CV analysis for three cycles (Figure S1) revealed that this oxidation is highly reversible, thus indicating that the resulting PTH-1 radical cation is quite stable. The photoluminescence maximum of PTH-1 was  $\sim 446$  nm (Figure 1B). From these data, the excited state reduction potential of PTH-1 was estimated to be  $E_{1/2}(\text{PTH-1}^{\bullet+}/\text{PTH-1}^*) = -2.1$  V, which is very similar to PTH and indicative of the highly reducing nature of these photocatalysts.

The synthesis of acrylamide-substituted PTH-2 is shown in Scheme 3. Nucleophilic aromatic substitution of 1-fluoro-4-nitrobenzene with phenothiazine produced 10-(4-nitrophenyl)-phenothiazine in 85% isolated yield after recrystallization from ethanol. Next, the nitro group was reduced to an amine via exposure to hydrogen in the presence of Pd/C catalyst. After filtering off the Pd/C, the mixture was directly treated with acryloyl chloride and triethylamine to produce acrylamide functionalized PTH-2 in 92% isolated yield after column chromatography.

With PTH-2 in hand, we selected *N*-isopropylacrylamide (NIPAAM) as a comonomer for gel formation due to the good solubility of poly *N*-isopropylacrylamide (poly(NIPAAM)) in many organic solvents and its lower critical solution temperature (LCST) behavior in water.<sup>57,58</sup> In the event, NIPAAM was copolymerized with PTH-2 and *N,N'*-methylenebis(acrylamide) (MBAA) (molar ratio of NIPAAM/PTH-2 = 30/1) at 70 °C using azobis(isobutyronitrile) (AIBN) as a free radical initiator (see Supporting Information for experimental details). The afforded material (Gel-PTH) was extracted with dimethylformamide (DMF) at least five times to remove unreacted monomers. Proton nuclear magnetic resonance (<sup>1</sup>H NMR) spectroscopy and gas chromatography (GC) analysis of the concentrated DMF extracts indicated that the conversions of both NIPAAM and PTH-2 were above 98%.

We next evaluated the swelling behavior of Gel-PTH in various solvents. As expected, the material swells without

Scheme 3. Synthesis of the Gel-PTH



dissolution in water and other organic solvents (e.g., MeCN, DMF, DMSO); the equilibrium swelling ratios (red columns, Figure 2) range from 2.8 (in MeCN) to 5.7 (in DMF) for these

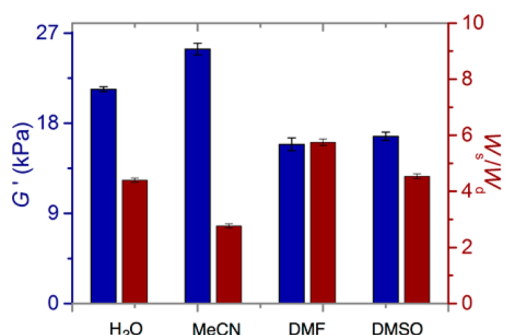


**Figure 2.** Mechanical characterization of Gel-PTH. Blue column: storage moduli ( $G'$ ) at 1 rad/s of Gel-PTH swollen to equilibrium in various solvents as measured by frequency sweeps in oscillatory rheometry; red column: equilibrium swelling ratios of Gel-PTH in various solvents.  $W_s$  = weight of swollen sample,  $W_d$  = weight of dry sample.

solvents. The storage moduli ( $G'$ ) (blue columns in Figure 2, also see Figure S2) as measured by oscillatory rheometry for these samples ranged from 15.8 kPa (in DMF) to 25.4 kPa (in MeCN). These differences reflect the network concentration in the various solvents: the most swollen material (in DMF) has the lowest network concentration and therefore should have the lowest  $G'$ . Notably, in each of these solvents, these materials are stiff enough to be easily handled without breaking, which is critical for simple catalyst removal.

Gel-PTH is 86% poly(NIPAAm) by mass, and thus we expected it should display LCST behavior.<sup>57,58</sup> In polymers that display LCST behavior, above the LCST the entropic penalty of polymer solvation outweighs favorable enthalpic interactions with solvent, thus causing the polymer to become insoluble. We reasoned that this switch from the soluble/swollen state to the insoluble/collapsed state could offer a temperature-dependent external switch for CRP. To demonstrate that Gel-PTH does indeed display LCST behavior, we measured  $G'$  of water-swollen samples as a function of temperature. As shown in Figure 3A, when the temperature was raised from 20 to 50 °C,  $G'$  increased nearly 5 times from ~21 kPa to ~110 kPa, which is indicative of the LCST transition.<sup>57,58</sup> Furthermore, this behavior was highly reversible as shown by the changes in  $G'$  and the loss modulus ( $G''$ ) when the temperature was cycled between 20 and 50 °C five times. Finally, optical images of the water swollen Gel-PTH at 20 and 50 °C (Figure 3B) show that the material not only shrinks upon heating, but also undergoes a transparent-to-opaque transition. Thus, at room temperature

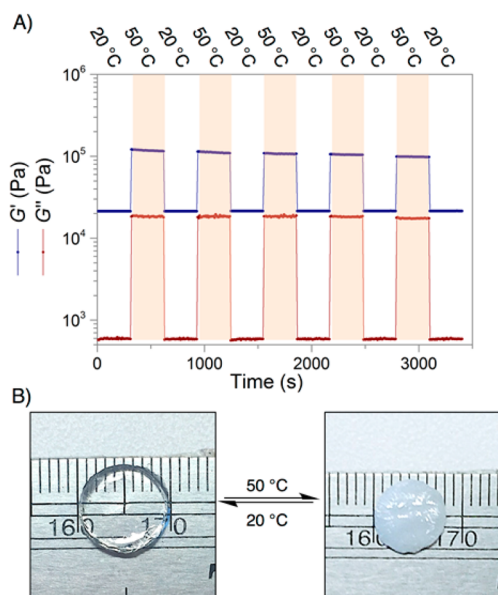


**Figure 3.** LCST behavior of water-swollen Gel-PTH. (A) Storage moduli ( $G'$ ) and loss moduli ( $G''$ ) of water-swollen Gel-PTH measured over five heating and cooling cycles; (B) optical images of water-swollen Gel-PTH before and after heating.

in water, the gel is transparent and highly swollen, which should allow for initiators, monomers, and macromolecules to diffuse into the network during photo-CRP and be activated by photoinduced electron transfer; such diffusion is well-established in gels prepared via free radical polymerization, which have large heterogeneous pores.<sup>59–61</sup> Above the LCST, the gel expels solvent and becomes opaque, which should preclude photo-CRP or at least limit it to the gel surface where it would be much less efficient. Therefore, such a system could enable “AND” Logic-CRP with two external controls: light of an appropriate wavelength and a specific temperature range.

**2. Gel-PTH Catalyzed Photo-CRP.** Having demonstrated the synthesis and LCST behavior of Gel-PTH, we next turned to investigating the applicability of this responsive material as a switchable heterogeneous catalyst for photo-CRP.

We first performed “ON”/“OFF” experiments for the polymerization of NIPAAm from TTC-1 in MeCN at room temperature by periodically switching the CFL light source. As shown in Figure 4A, after an induction period, the NIPAAm monomer conversion and  $M_n$  increased during the first “ON” cycle. When the reaction was kept in the dark for 60 min, there was no further increase in conversion or  $M_n$ . Exposing the reaction mixture to light for another 2 h led to increased conversion and  $M_n$ . Similar results were obtained for second and third “ON”/“OFF” cycles. The data presented in Figure 4A



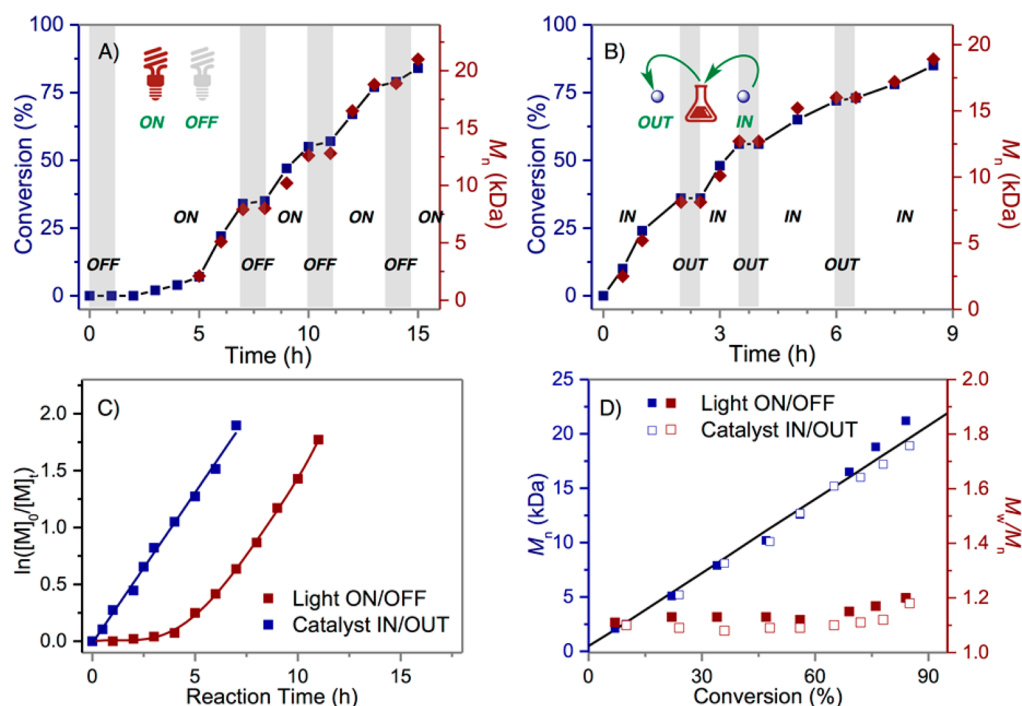


**Figure 4.** Gel-PTH catalyst enables external control of photo-CRP from TTC-1 in organic solvent. (A) light “ON”/“OFF” controlled polymerization of NIPAAM in MeCN; (B) catalyst “IN”/“OUT” controlled polymerization of NIPAAM in MeCN; (C) Reaction time vs  $\ln([M]_0/[M]_t)$ , with  $[M]_0$  and  $[M]_t$  being the concentration of monomers at time points 0 and  $t$ , respectively; (D) % conversion vs  $M_n$  and % conversion vs  $M_w/M_n$ .

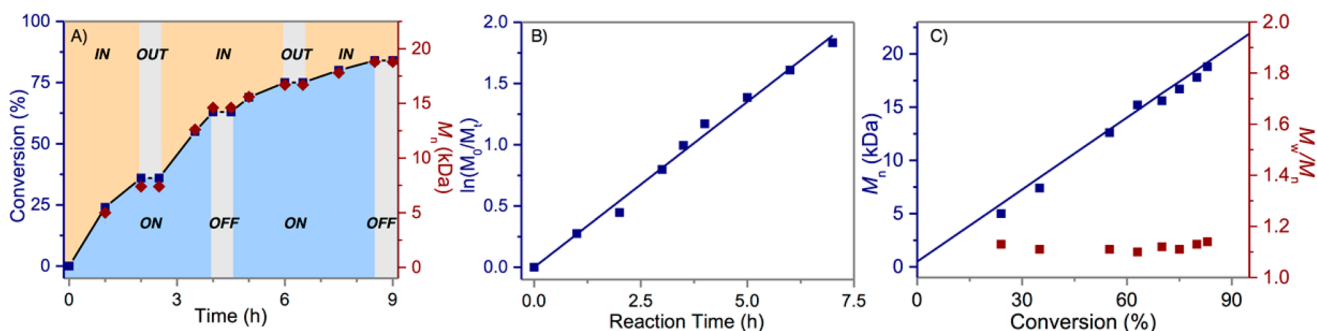


**Figure 5.** “AND” Logic-CRP enabled by Gel-PTH catalyst. (A) Light “ON”/“OFF” and catalyst “IN”/“OUT” controlled polymerization; (B) Reaction time vs  $\ln([M]_0/[M]_t)$ , with  $[M]_0$  and  $[M]_t$  being the concentration of monomers at time points 0 and  $t$ , respectively; (C) % conversion vs  $M_n$  and % conversion vs  $M_w/M_n$ .

demonstrates that Gel-PTH is an effective light-switchable photoredox catalyst for photo-CRP from TTC-1.

Nature switches “ON” and “OFF” biopolymer synthesis in response to the presence of suitable nutrients (e.g., amino acid monomers). This switching mechanism can be mimicked in photo-CRP by simply cycling a reagent “IN”/“OUT” of the reaction mixture. Such an approach would be quite difficult in a homogeneous system; the mechanically robust Gel-PTH offers a simple means to achieve such switching through simple removal and readdition of the gel photoredox catalyst. In these experiments, Gel-PTH was dried under inert atmosphere, and the material was then carefully immersed in or removed from an MeCN solution of NIPAAM (1.5 M) and TTC-1 (7.5 mM) under an  $N_2$  atmosphere and continuous light irradiation using a tweezers. As shown in Figure 4B, the NIPAAM conversion as well as  $M_n$  increased together in the presence of Gel-PTH (catalyst “IN”). After removing Gel-PTH, no further monomer conversion or change in  $M_n$  was detected in the following 30 min (catalyst “OUT”), even though the reaction mixture was

continuously exposed to light. By reimmersing the catalyst material into the reaction, the polymerization was effectively turned on, as proven by the increase in monomer conversion and  $M_n$ . The following two cycles of catalyst “IN”/“OUT” experiments demonstrated the reliability of this method for gaining switchable control over photo-CRP.

It should be noted that in each of the above examples (Figure 4A and B), both the monomer conversion and  $M_n$  increased simultaneously during every cycle when the reaction was turned “ON” via either light or catalyst presence. These findings suggest that each stimulus induces the reinitiation of existing polymer chains as opposed to the alternative possibility that they initiate the growth of new chains during each cycle. Thus, the polymerization displays living behavior that is distinct from classical photoinitiated free radical polymerizations.

Plots of  $\ln([M]_0/[M]_t)$  as a function of reaction time<sup>62</sup> (Figure 4C) and  $M_n$  as a function of monomer conversion (Figure 4D) demonstrate that Gel-PTH-catalyzed photo-CRP produces polymers with excellent control for both switching

methods. Following an induction period, linear relationships were observed for both  $\ln([M]_0/[M]_t)$  versus reaction time (Figure 4C) and  $M_n$  versus monomer conversion (Figure 4D). In Figure 4C, an induction period was observed in the light-controlled case (red line) most likely due to the presence of air in the Gel-PTH catalyst prior to the polymerization, which was absent in the samples prepared in a glovebox and used for “IN”/“OUT” studies (blue line). Similar induction periods were observed in Boyer’s recent work with metal photocatalysts.<sup>35,36</sup> Notably, the slopes of  $\ln([M]_0/[M]_t)$  versus time (apparent propagation rate constant,  $k_p^{app}$ ) after the induction period were very similar (Figure 4C). For each method,  $M_w/M_n$  remained low (ca. 1.1–1.3) during the polymerization process (monomer conversion >80%). Gel permeation chromatography (GPC) traces of representative poly(NIPAAM) from TTC-1 obtained from the various switching experiments (Figure S3 and S4) are unimodal, which provides further evidence of the control achieved in this system.

To achieve Logic-CRP, we imagined that catalyst presence and light combined could serve as an “AND” gate for chain growth. As shown in Figure 5A, in the presence of both Gel-PTH and light irradiation, monomer (NIPAAM) conversion and  $M_n$  continuously increased. When either catalyst was “OUT” or light was “OFF”, the reaction was interrupted immediately as confirmed by no further increase in monomer conversion or  $M_n$ . The two triggers were periodically switched between catalyst “IN”/“OUT” and light “ON”/“OFF”. In each cycle, the polymerization was readily reinitiated or ceased as depicted in Figure 5A.

Plots of  $\ln([M]_0/[M]_t)$  versus reaction time<sup>62</sup> (Figure 5B) and  $M_n$  versus monomer conversion (Figure 5C) (for GPC traces see Figure S5) showed linear relationships and  $M_w/M_n$  remained low (1.09–1.15) throughout the entire process. Moreover, the slope of  $\ln([M]_0/[M]_t)$  versus time ( $k_p^{app} = 0.26$ ) was nearly the same as for reactions controlled with only light “ON”/“OFF” (Figure 4D, red line,  $k_p^{app} = 0.25$ ) or only catalyst “IN”/“OUT” (Figure 4D, blue line,  $k_p^{app} = 0.27$ ), indicating that these two switches can be integrated in one system without affecting the polymerization kinetics.

Having demonstrated one variation of “AND” Logic-CRP, we turned to exploiting the unique LCST behavior of Gel-PTH to achieve thermally controlled polymerization. In contrast to the examples above, which were conducted in MeCN solvent, the LCST property of Gel-PTH requires water as the solvent. Despite the great progress in photoredox catalyzed photo-CRP, there are relatively few examples wherein such reactions are conducted in aqueous media. The Matyjaszewski group reported visible light-induced ATRP with ppm-levels of Cu in aqueous media.<sup>21</sup> The Boyer group developed an aqueous Ru-catalyzed photopolymerization and applied this method in biological media.<sup>37</sup> In both examples, light was demonstrated to be an effective stimulus to achieve switchable chain growth through the use of “ON”/“OFF” experiments. With Gel-PTH, we envisioned using “LOW”/“HIGH” temperature as an additional control element to provide “AND” gating of photo-CRP through the use of light and heat.

Polymerization reactions were run under constant light irradiation with a CFL light bulb while the reaction temperature was cycled between 4 °C<sup>63</sup> and 50 °C. Dry Gel-PTH catalyst was initially swollen in a mixture of bis-acid trithiocarbonate (TTC-1, 0.023 mmol), NIPAAM (4.5 mmol), water (3 mL), and DMF (40  $\mu$ L, internal standard) before exposure to light. As shown in Figure 6A, at 4 °C, the monomer conversion and

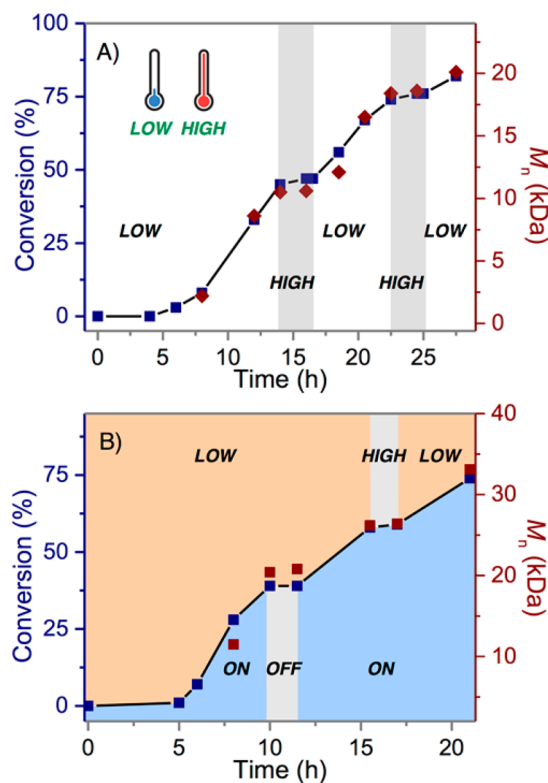


**Figure 6.** (A) Temperature “LOW”/“HIGH” controlled polymerization of NIPAAM in aqueous media; (B) “AND” Logic-CRP with Light “ON”/“OFF” and Temperature “LOW”/“HIGH” enabled by Gel-PTH catalyst.

number-average molar mass ( $M_n$ ) increased after an initial inhibition period. When the solution temperature was rapidly increased to 50 °C, where Gel-PTH undergoes a transparent-to-opaque transition within 2 min (see Supporting Information for experimental details of experimental setup), the monomer conversion was halted.<sup>64</sup> There was no significant increase in conversion or  $M_n$  when the reaction was kept at 50 °C for 60 min. Cooling back to 4 °C led to an opaque-to-transparent change within 2 min, and a further increase in monomer conversion and  $M_n$ . A second cycle of heating further confirmed the fidelity of the process (see Figure S6 for GPC traces,  $\ln([M]_0/[M]_t)$  vs reaction time and  $M_n$  vs conversion).

In the above experiment, the newly synthesized poly(NIPAAM) chains could also display LCST behavior, and thus perhaps the regulation of chain growth was not due to the LCST of Gel-PTH alone. To examine whether Gel-PTH could facilitate thermal-switching during the synthesis of a polymer that does not have a LCST in the same range, we next conducted the aqueous polymerization of poly(ethylene glycol) methyl ether acrylate (average  $M_n = 480$ , molar ratio of monomer/TTC-1 = 100/1) from TTC-1. In this system, we combined temperature and light as an “AND” gate for Logic-CRP. As shown in Figure 6B, light “ON” and temperature “LOW” controls led to monomer conversion and a continuous increase in  $M_n$ . When either light was “OFF” or temperature was “HIGH”, the polymerization was interrupted immediately as confirmed by no significant increase in monomer conversion or  $M_n$ . Plots of  $\ln([M]_0/[M]_t)$  versus reaction time and  $M_n$  versus monomer conversion showed linear relationships after an induction period (see Figure S7 for GPC traces,  $\ln([M]_0/[M]_t)$  vs reaction time and  $M_n$  vs conversion). While the values

Table 1. Polymerization of Acrylates and Acryl Amides from Trithiocarbonates with Gel-PTH Catalyst<sup>a</sup>

entry	monomer	initiator	molar ratio of monomer/initiator/PTH <sup>b</sup>	solvent	time (h)	conv. (%)	$M_{n,theory}$ (kDa)	$M_{n,GPC}$ (kDa)	$M_w/M_n$
1	NIPAAM	TTC-2	200/1/0	MeCN	12	<5	—	—	—
2	NIPAAM	TTC-2	200/1/0.1	MeCN	10	82	19.0	19.5	1.15
3	NIPAAM	TTC-2	500/1/0.25	MeCN	10	84	47.9	46.6	1.21
4	DMA	TTC-2	200/1/0.1	MeCN	10	81	16.5	17.4	1.11
5	nBA	TTC-2	250/1/0.1	MeCN	24	78	25.4	26.7	1.09
6	MA	TTC-2	200/1/0.1	MeCN	24	80	14.2	15.3	1.10
7	EGMEA	TTC-2	250/1/0.1	MeCN	16	80	26.5	27.7	1.09
8	NIPAAM	TTC-3	200/1/0.1	MeCN	10	83	19.2	21.2	1.16
9	NIPAAM	TTC-3	200/1/0	DMSO	12	<5	—	—	—
10	NIPAAM	TTC-3	200/1/0	DMF	12	<5	—	—	—
11	NIPAAM	TTC-3	200/1/0.1	DMSO	8	91	21.0	24.6	1.20
12	NIPAAM	TTC-3	200/1/0.1	DMF	10	81	18.7	17.6	1.29
13	HEA	TTC-3	250/1/0.1	DMSO	9	91	26.1	27.9	1.24
14 <sup>c</sup>	HEA	TTC-3	200/1/0.1	DMSO	12	85	20.2	19.8	1.20
15	MA	TTC-3	200/1/0.1	DMSO	10	89	15.7	16.6	1.15
16	DMA	TTC-4	200/1/0.1	MeCN	12	80	14.1	14.8	1.07
17	tBA	TTC-4	200/1/0.1	MeCN	12	82	21.3	21.4	1.19

<sup>a</sup>Reaction conditions: monomer (1.5 M), the molar ratio of monomer/iniferter/PTH was as shown in the table, room temperature, a 14 W CFL bulb was used for irradiation.  $M_n$  = number-average molar mass;  $M_w$  = weight-average molar mass. The conversion of monomer was determined by <sup>1</sup>H NMR spectroscopy.  $M_{n,theory}$  was calculated according to the monomer conversion.  $M_{n,GPC}$  and  $M_w/M_n$  were determined by GPC analysis. <sup>b</sup>The molar ratio of catalyst is calculated according to the PTH unit content contained in the Gel-PTH added into the reaction. <sup>c</sup>LED ( $\lambda_{max}$  = 410 nm) light is used.

Table 2. Polymerization of Vinyl Acetate and N-Vinylpyrrolidone with Gel-PTH Catalyst<sup>a</sup>

entry	monomer	initiator	molar ratio of monomer/initiator/PTH <sup>b</sup>	time (h)	conv. (%)	$M_{n,theory}$	$M_{n,GPC}$	$M_w/M_n$
1	VAc	TTC-3	100/1/0.1	24	0	—	—	—
2	VAc	TTC-4	100/1/0.1	24	0	—	—	—
3	VAc	Xanthate	100/1/0	24	0	—	—	—
4	VAc	Xanthate	100/1/0.1	14	30	2.8	2.9	1.12
5	VAc	Xanthate	100/1/0.1	32	80	7.1	7.7	1.15
6	VAc	Xanthate	200/1/0.1	32	75	13.1	14.9	1.16
7	NVP	Xanthate	100/1/0.1	40	35	4.1	4.6	1.26
8	NVP	Xanthate	100/1/0.1	84	72	8.2	9.0	1.32

<sup>a</sup>Reaction conditions: monomer (1.5 M), the molar ratio of monomer/iniferter/PTH was as shown in the table, in DMSO, at room temperature, a 14 W CFL bulb was used for irradiation. The conversion of monomer was determined by <sup>1</sup>H NMR spectroscopy.  $M_{n,theory}$  was calculated according to the monomer conversion.  $M_{n,GPC}$  and  $M_w/M_n$  were determined by GPC analysis. <sup>b</sup>The molar ratio of PTH is calculated according to the PTH unit content contained in the Gel-PTH added into the reaction.

of  $M_w/M_n$  for this aqueous polymerization ranged from 1.4 to 1.6 (ca.), no shoulder peaks were observed in the GPC traces. These data demonstrate another “AND” Logic-CRP enabled by Gel-PTH.

It should be noted that after long exposure to the aqueous reaction conditions used to produce the data shown in Figure 6, Gel-PTH became very soft and fragile. Thus, though it could be removed by filtration or centrifugation, it was not possible to perform simple “IN”/“OUT” experiments without the gel breaking apart. In the future, we plan to investigate increasing the mechanical properties of Gel-PTH in water by increasing the cross-linking density.

**3. Expanding Monomer Scope Using Gel-PTH as a Photoredox Catalyst for CRP.** Following our exploration of various photo-CRP switching methods enabled by Gel-PTH, we investigated the monomer, iniferter/initiator, and solvent scope of the Gel-PTH catalyst.

**3.1. Photoiniferter/RAFT Polymerization.** We first explored the scope of Gel-PTH for the growth of polymers from trithiocarbonate iniferters. We note that such reactions are often referred to as “PET-RAFT” whereas we prefer the name “photo-iniferter polymerization”; our choice of terminology is

due to the proposed mechanism of simultaneous reversible activation/deactivation and degenerative chain transfer, which are reflected in the iniferter concept.<sup>3,16</sup> In contrast, classical RAFT operates entirely via degenerative chain transfer, without reversible activation steps. Regardless of terminology, this reaction provides a robust methodology for the controlled synthesis of polymers using metal-free conditions and visible light. As shown in Table 1, in the absence of a photocatalyst, less than 5% monomer conversion was detected using photoiniferters TTC-2 or TTC-3 with different solvents such as MeCN, dimethyl sulfoxide (DMSO), or DMF using a 14 W CFL light source (entries 1, 9 and 10). Though Qiao and co-workers have reported that analogous TTCs can be directly activated by visible light,<sup>65</sup> we have not observed similar phenomena under the conditions used in our studies. When the Gel-PTH catalyst containing 0.05 mol % of PTH relative to NIPAAM was added into the reaction mixture, 82% of NIPAAM monomer in solution was polymerized in 10 h, producing poly(NIPAAM) with 19.5 kDa molar mass, which is in accordance with the theoretical molar mass estimated based on conversion and the molar ratio of monomer/iniferter (entry 2). When a 500/1 molar ratio of NIPAAM/TTC-2 was used,

Table 3. Polymerization of Methacrylates from EBP with Gel-PTH Catalyst<sup>a</sup>

entry	monomer	molar ratio of monomer/initiator/PTH <sup>b</sup>	time (h)	conv. (%)	$M_{n,theory}$ (kDa)	$M_{n,GPC}$ (kDa)	$M_w/M_n$
1	MMA	100/1/0	26	<5	—	—	—
2	MMA	100/1/0.05	26	29	3.1	3.8	1.26
3	MMA	100/1/0.1	26	56	5.8	6.1	1.21
4	MMA	120/1/0.1	40	80	9.8	10.6	1.31
5 <sup>c</sup>	MMA	100/1/0.1	56	82	8.4	8.9	1.42
6	MtBA	100/1/0.1	26	60	8.8	9.2	1.25
7	MtBA	100/1/0.1	40	82	11.1	10.5	1.36

<sup>a</sup>Reaction conditions: monomer (1.5 M), the molar ratio of monomer/EBP/PTH was as shown in the table, in DMSO, at room temperature, a 14 W CFL bulb was used for irradiation. The conversion of monomer was determined by <sup>1</sup>H NMR spectroscopy.  $M_{n,theory}$  was calculated according to the monomer conversion.  $M_{n,GPC}$  and  $M_w/M_n$  were determined by GPC analysis. <sup>b</sup>The molar ratio of PTH is calculated according to the PTH unit content contained in the Gel-PTH added into the reaction. <sup>c</sup>LED ( $\lambda_{max}$  = 410 nm) light is used.

the molar mass of the polymer increased to 46.6 kDa with  $M_w/M_n$  = 1.21 while the monomer conversion was similar (entry 3). Analogous polymerizations of other acrylamides and acrylates, such as *N,N*-dimethylacrylamide (DMA), *n*-butyl acrylate (nBA), methyl acrylate (MA), and ethylene glycol methyl ether acrylate (EGMEA) gave the corresponding polymers in good conversions (entries 4 to 7). The molecular weights determined by <sup>1</sup>H NMR were in very good agreement with the theoretical values (Figures S8 and S9).

With TTC-3, Gel-PTH catalyzed photo-CRP of acrylamides and acrylates (entries 11 to 15) in either DMSO or DMF produced polymers with narrow molar mass distributions ( $M_w/M_n$  < 1.30) at high conversions (>80%). Similar results were obtained by irradiation with a blue LED light ( $\lambda_{max}$  = 410 nm) as the irradiation source rather than a CFL bulb (entry 14). Photo-CRP with Gel-PTH and unsymmetrically substituted trithiocarbonate TTC-4 also provided excellent control over polymer molar mass distribution ( $M_w/M_n$  < 1.20) for the polymerization of DMA and *t*-butyl acrylate (tBA).

Analogous polymerizations of vinyl acetate (VAc) and *N*-vinylpyrrolidone (NVP) were conducted as outlined in Table 2. When TTC-3 and TTC-4 were used as the photoinitiators, no monomer conversion was observed. When Xanthate was used, VAc was efficiently polymerized. By controlling the reaction time and the molar ratio of monomer/initiator, poly(VAc) of different molar masses was produced with  $M_w/M_n$  = 1.12–1.16 (entries 4 to 6). <sup>1</sup>H NMR analysis showed good agreement between the molar mass and the end group fidelity for poly(VAc) (Figure S10). This method also allowed the photo-CRP of NVP under visible light irradiation, as shown in entries 7 and 8.

**3.2. Photo-ATRP.** We next explored the photo-ATRP of methacrylates using ethyl 2-bromopropionate (EBP) as an initiator. As shown in Table 3, without a photo catalyst, < 5% conversion of methyl methacrylate (MMA) was detected (entry 1). When Gel-PTH was added, photo-CRP was realized; varying the irradiation time produced PMMA of different  $M_n$  (from 3.8 kDa to 8.4 kDa) with good control of molar mass distributions ( $M_w/M_n$  = 1.21–1.31, entries 2 to 4). Furthermore, this method was successful for the polymerization of *t*-butyl methacrylate (MtBA). Both poly(MMA) and poly(MtBA) were analyzed by <sup>1</sup>H NMR (Figure S11) and the obtained  $M_n$  values agreed with the values estimated by GPC analysis and monomer conversion.

**4. Synthesis of Block Copolymers from Macro-Iniferters using Gel-PTH Photoredox Catalyst.** To assess whether Gel-PTH catalyzed photo-CRP could be used to produce block copolymers from macro-iniferters, we conducted

a series of chain extension experiments. First, poly(DMA) was synthesized using photo-CRP of DMA from TTC-3 with Gel-PTH catalyst. To validate its structure, <sup>1</sup>H NMR (Figure S12), GPC (Figure S13), MALDI-TOF (matrix-assisted laser desorption/ionization time-of-flight) mass spectroscopy (Figure S14), IR (Figure S15), and UV-vis (Figure S16) spectroscopy were conducted. The MALDI-TOF (Figure S13) spectrum exhibited a single set of peaks. The observed *m/z* values (e.g.,  $M_n$  = 5191 Da) are in good agreement with calculated values and with GPC analysis ( $M_n$  = 5289 Da,  $M_w/M_n$  = 1.09) and the  $M_n$  ( $M_n$  = 5252 Da) obtained from <sup>1</sup>H NMR. In a representative <sup>1</sup>H NMR spectrum (Figure 7A),

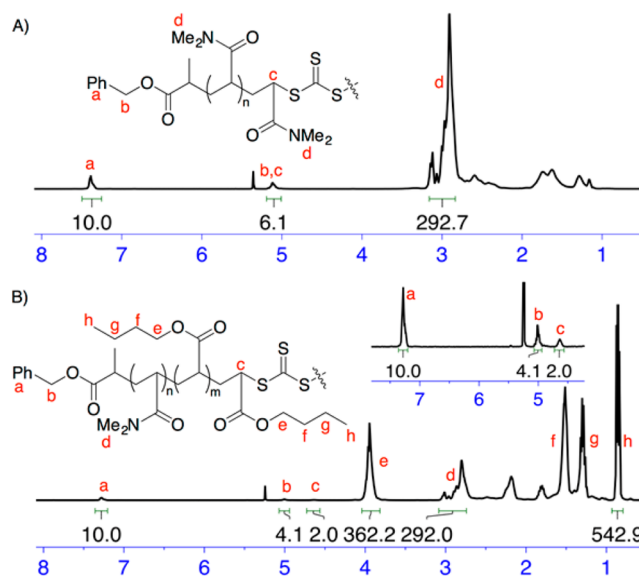


Figure 7. (A) <sup>1</sup>H NMR of poly(DMA); (B) <sup>1</sup>H NMR of poly(DMA)-*b*-poly(nBA)-*b*-poly(DMA). Note: only half of the structure is shown for this symmetrical A–B–A triblock copolymer.

resonances that correspond to the protons from the benzyl chain ends are observed at 7.40 and 5.11 ppm, indicating that this method provides excellent end group fidelity. Meanwhile, the FTIR peak at 1732 cm<sup>−1</sup> (Figure S15) and the UV-vis absorption at 310 nm (Figure S16), which are characteristic of the TTC unit, also confirmed the structure of the proposed macro-TTC.

With this macro-TTC, subsequent chain extensions were conducted with three different monomers including NIPAAm, nBA, and EGMEA. In these experiments, all of the resulting A–B–A triblock copolymers were isolated and analyzed via <sup>1</sup>H



NMR (Figures S17 to S19) and GPC. As exemplified by poly(DMA)-*b*-poly(nBA)-*b*-poly(DMA) in Figure 7B, the block copolymer product clearly shows the incorporation of the second monomer; an  $M_n$  of 28.2 kDa was calculated from  $^1\text{H}$  NMR analysis based on integration of the benzyl end groups relative to the polymer backbone. The GPC traces for three different block copolymers are shown in Figure 8. Narrow

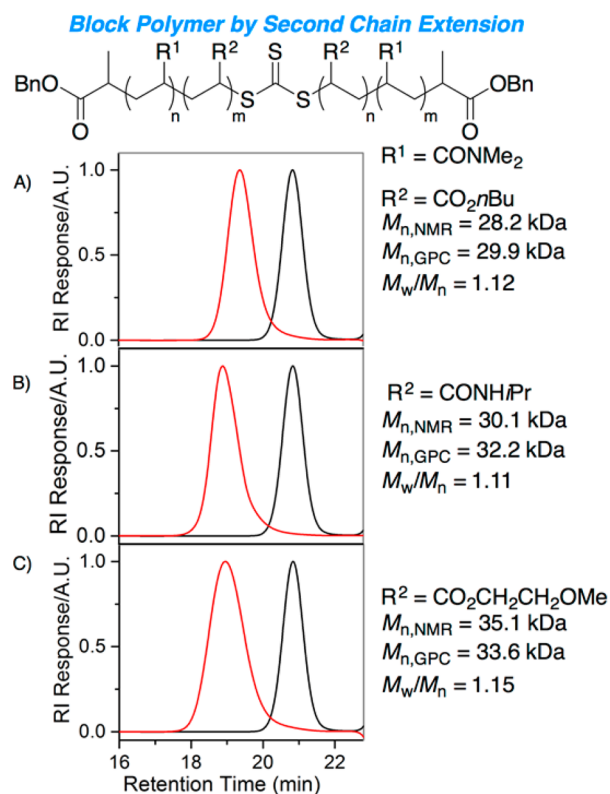


**Figure 8.** GPC traces of block copolymers synthesized with Gel-PTH, black trace = starting macro iniferter poly(DMA), red trace = block copolymer.

molecular weight distributions were obtained in all cases, and no low molar mass tailing is observed. Moreover, the estimated  $M_n$  values obtained via GPC are in good agreement with those calculated from  $^1\text{H}$  NMR.

**5. Gel-PTH Recycling.** Given that Gel-PTH is a heterogeneous catalyst and that, as shown above, it can be repeatedly added or removed from a photo-CRP reaction, we reasoned that it should be possible to recycle Gel-PTH thus enabling the synthesis of several batches of polymer using the same catalyst. We conducted catalyst-recycling experiments wherein Gel-PTH was removed from a completed photo-CRP reaction (in MeCN) with a tweezers, rinsed with MeCN, and used directly in another photo-CRP reaction in MeCN. As shown in Figure 9, when the same piece of Gel-PTH was used for six photo-CRP reactions all run for the same amount of time with extensive washing between each cycle ( $5 \times 10$  mL MeCN), the resulting polymer products had almost the same  $M_n$  (20.9–21.6 kDa) and  $M_w/M_n$  (1.13–1.16) values. GPC analysis (Figure S20) showed unimodal peaks with no low molar mass tailing. These experiments demonstrate the ease of recycling and the consistent performance of Gel-PTH as a catalyst for photo-CRP.

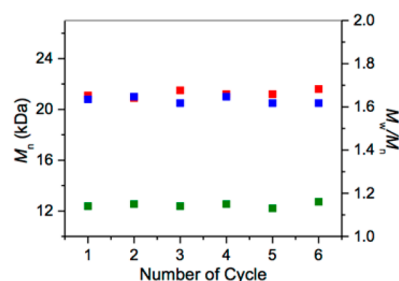


**Figure 9.** Recycling Gel-PTH catalyst in multiple photo-CRP reactions using NIPAAm monomer in MeCN. Red points represent  $M_{n,theory}$  values calculated from monomer conversion; blue points represent  $M_{n,GPC}$  values estimated by GPC analysis; green points represent  $M_w/M_n$  values.

## CONCLUSION

We have developed a thermally responsive gel-bound photo-redox catalyst—Gel-PTH—that was obtained via a simple three-step synthesis. Gel-PTH enabled robust switching of photo-CRP reactions in response to temperature, light, and catalyst presence, which is, to our knowledge, the first example of multistimuli-switching of photo-CRP using a single catalyst and three different triggers. Gel-PTH also enabled the integration of different controls: (1) light “ON”/“OFF” and catalyst “IN”/“OUT”, and (2) light “ON”/“OFF” and temperature “LOW”/“HIGH”, to achieve “AND” gating of CRP, i.e., Logic-CRP. The advantages of this new catalyst lie in (1) its high transparency enabled by the solvent swollen gel architecture and the lack of any metals; (2) its heterogeneous nature and robust mechanical properties realized through the cross-linked polymer network; (3) its LCST behavior achieved via the use of poly(NIPAAm). Both photoiniferter/RAFT and ATRP reactions were realized using corresponding iniferters/initiators, which enabled the photo-CRP of a wide range of monomers including acrylates, methacrylates, acrylamides, vinyl esters and vinyl amides. Demonstrations of block copolymer synthesis and catalyst-recycling further highlight the reliability and performance of this catalyst. Given the vast applications of heterogeneous catalysts as well as photochemistry in the chemical industry, energy, medicine, and defense, and the expanding interest in complex multiswitchable biomimetic reactions, we anticipate that our gel-bound photocatalyst approach will offer new opportunities for photocontrolled polymerization and potentially organic synthesis.

## ASSOCIATED CONTENT

### Supporting Information

The Supporting Information is available free of charge on the ACS Publications website at DOI: 10.1021/jacs.6b10345.

Materials, experimental procedures, characterization methods and additional figures (PDF)

## AUTHOR INFORMATION

### Corresponding Author

\*jaj2109@mit.edu

### ORCID

Jun Lin: 0000-0002-2087-6013

Jeremiah A. Johnson: 0000-0001-9157-6491



## Present Address

<sup>†</sup>State Key Laboratory of Molecular Engineering of Polymers, Department of Macromolecular Science, Fudan University, Shanghai 200433, China.

## Notes

The authors declare no competing financial interest.

## ■ ACKNOWLEDGMENTS

We thank the National Science Foundation (CHE-1334703) for support of this work.

## ■ REFERENCES

- (1) Leibfarth, F. A.; Mattson, K. M.; Fors, B. P.; Collins, H. A.; Hawker, C. J. *Angew. Chem., Int. Ed.* **2013**, *52*, 199–210.
- (2) Teator, A. J.; Lastovickova, D. N.; Bielawski, C. W. *Chem. Rev.* **2016**, *116*, 1969–1992.
- (3) Chen, M.; Zhong, M.; Johnson, J. A. *Chem. Rev.* **2016**, *116*, 10167–10211.
- (4) Dadashi-Silab, S.; Doran, S.; Yagci, Y. *Chem. Rev.* **2016**, *116*, 10212–10275.
- (5) Yagci, Y.; Jockusch, S.; Turro, N. J. *Macromolecules* **2010**, *43*, 6245–6260.
- (6) Zivic, N.; Bouzrati-Zerelli, M.; Kermagoret, A.; Dumur, F.; Fouassier, J.-P.; Gigmes, D.; Lalevee, J. *ChemCatChem* **2016**, *8*, 1617–1631.
- (7) Magenau, A. J. D.; Strandwitz, N. C.; Gennaro, A.; Matyjaszewski, K. *Science* **2011**, *332*, 81–84.
- (8) Park, S.; Chmielarz, P.; Gennaro, A.; Matyjaszewski, K. *Angew. Chem., Int. Ed.* **2015**, *54*, 2388–2392.
- (9) Yoon, H. J.; Kuwabara, J.; Kim, J.-H.; Mirkin, C. A. *Science* **2010**, *330*, 66–69.
- (10) Gregson, C. K. A.; Gibson, V. C.; Long, N. J.; Marshall, E. L.; Oxford, P. J.; White, A. J. P. *J. Am. Chem. Soc.* **2006**, *128*, 7410–7411.
- (11) Broderick, E. M.; Guo, N.; Vogel, C. S.; Xu, C.; Sutter, J.; Miller, J. T.; Meyer, K.; Mehrkhodavandi, P.; Diaconescu, P. L. *J. Am. Chem. Soc.* **2011**, *133*, 9278–9281.
- (12) Wang, X.; Thevenon, A.; Brosmer, J. L.; Yu, I.; Khan, S. I.; Mehrkhodavandi, P.; Diaconescu, P. L. *J. Am. Chem. Soc.* **2014**, *136*, 11264–11267.
- (13) Biernesser, A. B.; Li, B.; Byers, J. A. *J. Am. Chem. Soc.* **2013**, *135*, 16553–16560.
- (14) Caruso, M. M.; Davis, D. A.; Shen, Q.; Odom, S. A.; Sottos, N. R.; White, S. R.; Moore, J. S. *Chem. Rev.* **2009**, *109*, 5755–5798.
- (15) Piermattei, A.; Karthikeyan, S.; Sijbesma, R. P. *Nat. Chem.* **2009**, *1*, 133–137.
- (16) Otsu, T.; Yoshida, M. *Makromol. Chem., Rapid Commun.* **1982**, *3*, 127–32.
- (17) Fors, B. P.; Hawker, C. J. *Angew. Chem., Int. Ed.* **2012**, *51*, 8850–8853.
- (18) Treat, N. J.; Fors, B. P.; Kramer, J. W.; Christianson, M.; Chiu, C.-Y.; Read de Alaniz, J.; Hawker, C. J. *ACS Macro Lett.* **2014**, *3*, 580–584.
- (19) Treat, N. J.; Sprafke, H.; Kramer, J. W.; Clark, P. G.; Barton, B. E.; Read de Alaniz, J.; Fors, B. P.; Hawker, C. J. *J. Am. Chem. Soc.* **2014**, *136*, 16096–16101.
- (20) Pan, X.; Lamson, M.; Yan, J.; Matyjaszewski, K. *ACS Macro Lett.* **2015**, *4*, 192–196.
- (21) Pan, X.; Malhotra, N.; Simakova, A.; Wang, Z.; Konkolewicz, D.; Matyjaszewski, K. *J. Am. Chem. Soc.* **2015**, *137*, 15430–15433.
- (22) Kwak, Y.; Matyjaszewski, K. *Macromolecules* **2010**, *43*, 5180–5183.
- (23) Konkolewicz, D.; Schroder, K.; Buback, J.; Bernhard, S.; Matyjaszewski, K. *ACS Macro Lett.* **2012**, *1*, 1219–1223.
- (24) Ribelli, T. G.; Konkolewicz, D.; Bernhard, S.; Matyjaszewski, K. *J. Am. Chem. Soc.* **2014**, *136*, 13303–13312.
- (25) Anastasaki, A.; Nikolaou, V.; Pappas, G. S.; Zhang, Q.; Wan, C.; Wilson, P.; Davis, T. P.; Whittaker, M. R.; Haddleton, D. M. *Chem. Sci.* **2014**, *5*, 3536–3542.
- (26) Anastasaki, A.; Nikolaou, V.; Zhang, Q.; Burns, J.; Samanta, S. R.; Waldron, C.; Haddleton, A. J.; McHale, R.; Fox, D.; Percec, V.; Wilson, P.; Haddleton, D. M. *J. Am. Chem. Soc.* **2014**, *136*, 1141–1149.
- (27) Frick, E.; Anastasaki, A.; Haddleton, D. M.; Barner-Kowollik, C. *J. Am. Chem. Soc.* **2015**, *137*, 6889–6896.
- (28) Tasdelen, M. A.; Ciftci, M.; Yagci, Y. *Macromol. Chem. Phys.* **2012**, *213*, 1391–1396.
- (29) Dadashi-Silab, S.; Atilla Tasdelen, M.; Mohamed Asiri, A.; Bahadar Khan, S.; Yagci, Y. *Macromol. Rapid Commun.* **2014**, *35*, 454–459.
- (30) Alfredo, N. V.; Jalapa, N. E.; Morales, S. L.; Ryabov, A. D.; Le Lagadec, R.; Alexandrova, L. *Macromolecules* **2012**, *45*, 8135–8146.
- (31) Telitel, S.; Dumur, F.; Telitel, S.; Soppera, O.; Lepeltier, M.; Guillaneuf, Y.; Poly, J.; Morlet-Savary, F.; Fioux, P.; Fouassier, J.-P.; Gigmes, D.; Lalevee, J. *Polym. Chem.* **2015**, *6*, 613–624.
- (32) Tasdelen, M. A.; Uygur, M.; Yagci, Y. *Macromol. Rapid Commun.* **2011**, *32*, 58–62.
- (33) Theriot, J. C.; Lim, C.-H.; Yang, H.; Ryan, M. D.; Musgrave, C. B.; Miyake, G. M. *Science* **2016**, *352*, 1082.
- (34) Zhou, H.; Johnson, J. A. *Angew. Chem., Int. Ed.* **2013**, *52*, 2235–2238.
- (35) Xu, J.; Jung, K.; Atme, A.; Shanmugam, S.; Boyer, C. J. *Am. Chem. Soc.* **2014**, *136*, 5508–5519.
- (36) Xu, J.; Jung, K.; Boyer, C. *Macromolecules* **2014**, *47*, 4217–4229.
- (37) Xu, J.; Jung, K.; Corrigan, N. A.; Boyer, C. *Chem. Sci.* **2014**, *5*, 3568–3575.
- (38) Shanmugam, S.; Boyer, C. J. *Am. Chem. Soc.* **2015**, *137*, 9988–9999.
- (39) Shanmugam, S.; Xu, J.; Boyer, C. J. *Am. Chem. Soc.* **2015**, *137*, 9174–9185.
- (40) Chen, M.; MacLeod, M. J.; Johnson, J. A. *ACS Macro Lett.* **2015**, *4*, 566–569.
- (41) McKenzie, T. G.; Fu, Q.; Wong, E. H. H.; Dunstan, D. E.; Qiao, G. G. *Macromolecules* **2015**, *48*, 3864–3872.
- (42) Chen, M.; Johnson, J. A. *Chem. Commun.* **2015**, *51*, 6742–5.
- (43) McKenzie, T. G.; Fu, Q.; Uchiyama, M.; Satoh, K.; Xu, J.; Boyer, C.; Kamigaito, M.; Qiao, G. G. *Adv. Sci.* **2016**, *3*, 1500394.
- (44) Shanmugam, S.; Xu, J.; Boyer, C. *Angew. Chem., Int. Ed.* **2016**, *55*, 1036–1040.
- (45) Fu, Q.; McKenzie, T. G.; Ren, J. M.; Tan, S.; Nam, E.; Qiao, G. G. *Sci. Rep.* **2016**, *6*, 20779.
- (46) Shanmugam, S.; Xu, J.; Boyer, C. *Polym. Chem.* **2016**, *7*, 6437–6449.
- (47) Zhao, Y.; Yu, M.; Zhang, S.; Wu, Z.; Liu, Y.; Peng, C.-H.; Fu, X. *Chem. Sci.* **2015**, *6*, 2979–2988.
- (48) Zhao, Y.; Yu, M.; Zhang, S.; Liu, Y.; Fu, X. *Macromolecules* **2014**, *47*, 6238–6245.
- (49) Nakamura, Y.; Arima, T.; Tomita, S.; Yamago, S. *J. Am. Chem. Soc.* **2012**, *134*, 5536–5539.
- (50) Yamago, S.; Ukai, Y.; Matsumoto, A.; Nakamura, Y. *J. Am. Chem. Soc.* **2009**, *131*, 2100–2101.
- (51) Ohtsuki, A.; Lei, L.; Tanishima, M.; Goto, A.; Kaji, H. *J. Am. Chem. Soc.* **2015**, *137*, 5610–5617.
- (52) Goto, A.; Scaiano, J. C.; Maretti, L. *Photochemical & Photobiological Sciences* **2007**, *6*, 833–835.
- (53) Wolpers, A.; Vana, P. *Macromolecules* **2014**, *47*, 954–963.
- (54) Asandei, A. D.; Adebolu, O. I.; Simpson, C. P. *J. Am. Chem. Soc.* **2012**, *134*, 6080–6083.
- (55) Koumura, K.; Satoh, K.; Kamigaito, M. *Macromolecules* **2009**, *42*, 2497–2504.
- (56) Hansch, C.; Leo, A.; Taft, R. W. *Chem. Rev.* **1991**, *91*, 165–195.
- (57) Kujawa, P.; Winnik, F. M. *Macromolecules* **2001**, *34*, 4130–4135.
- (58) Kaneko, Y.; Sakai, K.; Kikuchi, A.; Yoshida, R.; Sakurai, Y.; Okano, T. *Macromolecules* **1995**, *28*, 7717–7723.
- (59) Di Lorenzo, F.; Seiffert, S. *Polym. Chem.* **2015**, *6*, 5515–5528.
- (60) Kristin, E.; Curtis, W. F. *Biomed. Mater.* **2011**, *6*, 055006.

(61) Cruise, G. M.; Scharp, D. S.; Hubbell, J. A. *Biomaterials* **1998**, *19*, 1287–1294.

(62) Reaction time means the period when the trigger is switched “ON” to allow reacting.

(63) To quickly reach the opaque-to-transparent transformation below LCST, the reaction was conducted in a cold room at 4 °C.

(64) The LCST transition of the Gel material is accompanied with the phase transition of the produced poly(NIPAAm) in the reaction solution.

(65) McKenzie, T. G.; Fu, Q.; Wong, E. H. H.; Dunstan, D. E.; Qiao, G. G. *Macromolecules* **2015**, *48*, 3864–3872.